

Critical Collapse of the Exchange Enhanced Spin Splitting in 2-D Systems

¹D.R. Leadley, ²R.J. Nicholas, ³J.J. Harris and ⁴C.T. Foxon

¹ *Department of Physics, University of Warwick, Coventry, CV4 7AL, UK*

² *Department of Physics, Clarendon Laboratory, Parks Road, Oxford, OX1 3PU, UK*

³ *Department of Electronic and Electrical Engineering, University College, London, WC1E 7JE, UK*

⁴ *Department of Physics, Nottingham University, University Park, Nottingham, NG7 2RD, UK*

(Submitted to Phys. Rev. B May 11, 1998)

Abstract

The critical filling factor ν_c where Shubnikov-de Haas oscillations become spin split is investigated for a set of GaAs-GaAlAs heterojunctions. Finite temperature magnetoresistance measurements are used to extract the value of ν_c at zero temperature. The critically point is where the disorder potential has the same magnitude as the exchange energy, leading to the empirical relationship $\nu_c = g^* n_e \tau_s h / 2m_0$. This is valid for all the samples studied, where the density n_e and single particle lifetime τ_s both vary by more than an order of magnitude and g^* the exchange enhanced g -factor has a weak dependence on density. For each sample the spin gap energy shows a *linear* increase with magnetic field. Experiments in tilted magnetic field show the spin gap is the *sum* of the bare Zeeman energy and an exchange term. This explains why measurements of the enhanced g -factor from activation energy studies in perpendicular field and the coincidence method in tilted fields have previously disagreed.

73.40.Hm, 73.20.Dx, 72.20.Jv

I. INTRODUCTION

Quantisation of the Hall effect was first recognized in 1980 [1] and it is understood that plateaux appear in the off-diagonal component of the magnetoresistance tensor ρ_{xy} whenever the Fermi energy lies in a mobility gap of the electronic density of states. In an ideal sample this would be the cyclotron gap $\hbar\omega_c$. Associated with the plateaux are minima in the diagonal component which lead to the appearance of Shubnikov-de Haas oscillations (SdHO) in ρ_{xx} . SdHOs were observed in semiconductors as long ago as 1966 [2] and even in these earliest observations spin and valley splittings were seen to modify the underlying $1/B$ periodicity of the oscillations. In particular the spin splitting appeared to be much stronger than expected from just a bare Zeeman gap of $g_0\mu_B B$, leading to the idea of an enhanced g -factor g^* [3]. This enhancement is due to many-body electron interactions that are introduced by forming a widely separated electron-hole pair with reversed spin. It is often referred to as *exchange enhancement* (after the exchange-correlation terms encountered in Hartree Fock calculations) and leads to the spin gap being written as:

$$\Delta_{spin} = g^* \mu_B B = g_0\mu_B B + E_{ex}. \quad (1)$$

Notice particularly that this is the *sum* of the bare Zeeman energy and an exchange energy E_{ex} and that, unless $E_{ex} \propto B$, g^* will itself be a function of field as opposed to a simple multiple of g_0 . Several semi-empirical versions of this equation have been adopted to model experimental results but it is the calculation of E_{ex} that has particularly exercised theoreticians for the past thirty years [4–6].

It is now timely to revisit the exchange enhanced spin splitting for two reasons. First, there is currently great interest in complex spin textures, or skyrmions, at low odd integer filling factors ν [7]. This work has shown a rich spectrum of spin excitations and serves to remind us how poorly even the basic spin splitting is understood. The calculations indicate that at $\nu = 1$ skyrmion-antiskyrmion pairs will always have a lower excitation energy than electron-hole pairs, but for higher filling factors the preferred excitation depends crucially on how the force laws are treated for real systems both for single spin excitations and the larger textures [8]. Secondly, there is a prediction by Fogler and Shklovskii (FS) [6] that the exchange enhancement may be destroyed by disorder and lead to the collapse of the spin splitting at a critical filling factor ν_c . FS gives expressions for ν_c in terms of sample parameters relevant to GaAs/GaAlAs heterojunctions which can be compared with experiments [9,10].

These issues will be discussed further in the remainder of the paper, but first the phenomenon of spin splitting will be introduced with reference to some experimental data. The behavior as a function of temperature and sample parameters will then be investigated, both through the filling factor where the spin split SdH maxima appear and by considering the size of the energy gap at odd integer ν . The temperature dependence of the separation between the maxima is found to scale onto a universal curve for all filling factors and all samples in a way that suggests a phase transition. By understanding how ν_c varies with temperature we are able to extract the value at $T = 0$ from the finite temperature data, allowing meaningful comparison with theory. An empirical relationship between the critical filling factor and the measured sample parameters is established which justifies the idea of disorder driven collapse of the exchange enhancement. By measuring the energy gap at

different large odd filling factors within each sample we find a *linear* increase in Δ_{spin} with magnetic field. Although a \sqrt{B} increase would be expected for an exchange energy driven by the Coulomb energy, where correlation takes place over the magnetic length, this is not the case with multiple Landau levels (LL) occupied when the correlation length is set by the Fermi wavevector k_F and a linear behavior results. Finally, experiments in tilted field will be reported which show that the exchange part of Δ_{spin} depends only on the component of magnetic field perpendicular to the two-dimensional electron gas and that the increase in spin gap is due to the bare Zeeman term only. This explains why g -factors obtained from the coincidence method in tilted fields do not agree with those found from activation studies in perpendicular field [3,11].

II. THE SPIN SPLITTING PHENOMENON

The samples studied here are the well known GaAs/GaAlAs single heterojunctions grown at Philips Research Laboratories, Redhill having undoped spacer layer thickness in the range $100 \text{ \AA} < L_z < 3200 \text{ \AA}$. The samples cover a wide range of density and mobility and include examples with low disorder, which exhibit the fractional quantum Hall effect, as well as highly disordered samples, which have very wide integer quantum Hall plateaux. Table I lists some relevant sample parameters, measured at 1 K. The experiments consist of magnetoresistance measurements performed over a range of temperatures from 50 mK to 4.2 K with the magnetic field normal to the sample, except in the final section where we consider tilted field measurements. The temperature T is measured and stabilized using a ruthenium oxide resistor, mounted to be in thermal equilibrium with the sample and to have negligible magnetoresistance.

A typical low temperature recording of the diagonal resistivity ρ_{xx} for a high mobility sample G641 is shown in Fig. 1. At high magnetic fields, in this case $B > 0.5T$, the SdHOs are spin split and the maxima are evenly spaced, appearing at all half-integer filling factors. At low field, $B < 0.15T$ in Fig. 1, the maxima are again evenly spaced but here there is no spin splitting so they appear at odd integer filling factors. By examining either of these regions in isolation it would be impossible to tell whether or not the SdHOs were spin split without additional information. In the intermediate region, whose extent depends on the temperature of the measurement, the spin splitting is partially resolved. In this region, the spin split minima are less deep than those due to cyclotron splitting since their energy gaps are smaller. Also towards lower magnetic fields the spin split maxima converge with a rapid change from a spacing $\delta\nu = |\nu_{\uparrow} - \nu_{\downarrow}| = 1$ at high fields to $\delta\nu = 0$ where the spin splitting disappears. In Fig. 1, spin splitting can clearly be seen at $\nu = 23$ and at higher magnification it can just be made out for the next two peaks but no more. Clearly this is only a qualitative judgement of ν_c whereas a quantitative definition is required. In FS this was taken to be the point where $\delta\nu = 0.5$ at $T = 0$. Although the zero temperature requirement simplifies the theory, it adds complications when one only has experimental results at finite temperature as can be seen in Fig. 2. Data from several temperatures are re-plotted as a function of filling factor, allowing the convergence of the maxima to be seen more clearly. While the last spin split peak is at $\nu = 25$ in the 90 mK data, by 600 mK it appears at more than twice the magnetic field at $\nu = 9$. One aspect of this paper will be to establish a reliable way of extrapolating the real experimental data to the ideal $T = 0$ situation.

Let us now examine some differences between the regular SdHOs and the spin splitting by again referring to the magnetic field dependence shown in Fig. 1. The SdHOs are damped exponentially towards low field according to the well known Lifshitz-Kosevich formula [12]:

$$\Delta\rho_{xx} \propto \frac{X}{\sinh X} \exp\left(-\frac{\pi}{\omega_c\tau_s}\right) \cos(\pi(\nu + 1/2)), \quad (2)$$

where the factor containing $X = 2\pi^2kT/E_g$ arises from the width of the Fermi function at finite temperature. When there is no spin splitting the gap E_g is the cyclotron energy $\hbar\omega_c$. Eq. (2) shows that the damping at $T = 0$ is just determined by the single particle scattering time τ_s , but is larger at higher temperatures when the Fermi function becomes smeared. In practice this means that more SdHOs will be seen if the experiments are performed at lower temperatures and with higher resolution. Thus there is not a maximum filling factor ν_c^{SdH} at zero temperature and even when the LL broadening is significantly larger than $\hbar\omega_c$ small oscillations will still occur in the conductivity. However, the exponential damping will set a limit in a real experiment where the last oscillation observed is determined by experimental noise. Practically, great care also has to be taken to sweep the magnetic field sufficiently slowly and to obtain enough data points per oscillation. In our imperfect noisy experiments, SdHOs have been regularly observed at filling factors in excess of 100 and in the best cases with $\nu > 150$. Values of τ_s deduced from Eq. (2) are included in Table I.

The spin splitting disappears in quite a different way. If the minima at odd ν just became unresolved at a certain field, it could be argued that the signal was becoming lost in the noise due to an exponential term, with a damping factor different from that of the regular SdHOs. In this case spin splitting would be seen at lower fields (higher ν) if the experiment were performed more carefully. However, this does not appear to be the case and, in addition, there is a finite field where the maxima from either side of a spin split minimum converge, irrespective of the amount of experimental noise or resolution. This is a sign that the collapse is critical, indicative of a second order phase change when the exchange interaction is turned off. The position of the phase change is however dependent both on the sample and on the temperature. A dramatic example of the critical collapse may be seen for the higher density and more disordered sample G590 in Fig. 3. Here $\nu_c = 11$ which is at a much higher magnetic field than for G641 (14 times greater), and shows only a very weak temperature dependence, changing from $\nu_c = 11$ at 40 mK to $\nu_c = 9$ at 900 mK. This is however still a high quality sample as can be seen in the insert where the SdHOs are observed down to very low fields and only disappear into the noise below 0.2 T at around $\nu = 70$.

The collapse of the spin splitting can be studied in at least three different ways: as a function of magnetic field at fixed temperature (preferably 0 K), as discussed above; for a given SdH peak (of Landau level N [13]) as function of temperature at fixed field, as will be discussed below; or as a function of density for a given SdH peak at fixed temperature. We will only consider the first two cases.

Wong *et al.* [9] used gated samples to study the density dependence and found that for each N there was a critical density below which the splitting disappeared consistent with a phase change. In their data, the density where $\delta\nu_N = 0.5$ increased with the temperature of the measurement. By fitting their data in the range $0.5 < \delta\nu_N < 0.9$ and extrapolating to $\delta\nu_N = 0$ a critical density n_c was found for each N which allowed data from all peaks to

be scaled onto a single curve for each sample. Their results show that to first order $n_c \propto N$ which means that there was a critical magnetic field at which the spin splitting collapsed and the effect of varying the density was to align different filling factors with this critical field. This is exactly what would be expected if disorder destroys the exchange enhancement whose energy scale is set by the magnetic field. The critical field also varied between the samples, presumably in line with the disorder. However, it would appear that changing density had little effect on the disorder, as otherwise the critical field would change with density and there would not be linear relationship between N and n_c . Hence, the vertical axis of the phase diagram depicted in Fig. 4 of Ref. [9] is actually a measure of the spin gap size and not the disorder.

III. TEMPERATURE DEPENDENCE OF SPIN SPLITTING

We will now consider how the spin splitting at a particular filling factor can be observed to collapse as a function of temperature. Again it appears to be a critical phenomenon. The temperature evolution of the resistivity around $\nu = 15$ for sample G902 is shown in Fig. 4. (This example is chosen as it shows the fully resolved spin split minimum at low temperature changing to a maximum by 1 K.) At the lowest temperatures the two maxima can be seen at $\nu = 15 \pm 0.4$ and as the temperature is increased these remain at the same filling factor while the minimum becomes shallower. Only when the depth of the minimum is $< 10\%$ of the peak height do the maxima start to converge and then they do so rapidly as $\delta\nu$ collapses. It will also be noticed that once less than 0.5, $\delta\nu$ becomes difficult to measure reliably as the peak has a rather flat top. Figure 5 illustrates the actual filling factors at which maxima occur for each temperature (this time for sample G640 but all the samples behave similarly). The dotted lines on this figure show the positions expected when the spin splitting is either completely resolved or completely absent. By their convergence, the points clearly show transitions between these two limiting cases at different temperatures for each filling factor. Figure 5 thus represents the temperature driven phase diagram for sample G640 with the spin resolved phase to the lower left side of the figure. The dashed line on the figure, drawn through the positions where $\delta\nu = 0.5$, defines the phase boundary.

The separation of the individual spin split maxima is displayed as a function of temperature in Fig. 6 for odd filling factors in the range $19 > \nu > 9$ from sample G902. For each filling factor the collapse looks to be quite similar but occurs at a different temperature. At lower filling factors there is no noticeable change in $\delta\nu$ in the temperature range of the experiment, although there would again be a collapse at higher temperature. If the spin gap had just one component that increased with magnetic field then it should be possible to collapse the data of Fig. 6 onto a single curve as a function of a scaled temperature i.e. $\delta\nu(T/T_\nu)$ with a T_ν determined for each filling factor. However, the data does not scale in this way. This can be seen by looking at the maximum value of $\delta\nu$, which would be 1.0 at $T = 0$ for all ν if $\delta\nu$ were a function of T/T_ν , but in fact decreases at higher ν . Instead, the data can be collapsed by simply shifting the temperature axes, i.e. plotting it as $\delta\nu(T') = \delta\nu(T - T_{0.5})$ in Fig. 7, where $T_{0.5}$ is the temperature where $\delta\nu = 0.5$ for each filling factor. $T_{0.5}$ is used in preference to the temperature where $\delta\nu = 0$ as it is both experimentally accessible and corresponds to the mid-point of the gap's collapse. No fitting of the data is required so we do not have to assume any functional form to the collapse of

the gap, we just read off $T_{0.5}$ at each filling factor from Fig. 6. The remarkable behavior shown in Fig. 7 demonstrates that the gap collapses over the same range of temperature for all filling factors. In other words there is a single finite width to the phase boundary. This suggests that once there is sufficient thermal energy to initiate a collapse (which increases with magnetic field) the same amount of additional thermal energy will complete the phase transition at all magnetic fields. Other samples show a similar behavior but with the transition occurring over a smaller temperature range in higher mobility samples, i.e. the width of the phase boundary decreases as the mobility increases. Indeed it is possible to collapse the data for all the samples (and all filling factors) onto a single curve by normalizing $T - T_{0.5}$ by a sample dependent temperature T_0 as shown in Fig. 8. The value used for T_0 is found by fitting the data for each sample to $\delta\nu = 0.5 + a_1(1 - \exp((T - T_{0.5})/T_0))$, which is the simplest function that provides a reasonable fit the data. Similar values of T_0 , but slightly lower quality fits, can be obtained from a modified Brillouin function, as used in Ref. [9], $\delta\nu = a \coth(2a(T - T_{0.5} - T_0)/T_0) - b \coth(2b(T - T_{0.5} - T_0)/T_0)$. At present we do not understand the physical significance of either of these functional forms, merely using them to extract T_0 , but we do note that T_0 is a good measure of the temperature range over which the transition proceeds. Figure 9 shows how T_0 varies with disorder in the samples, where the degree of disorder is represented by the inverse quantum lifetime $1/\tau_s$, measured from the low field SdHOs in each sample. This assumes that the SdHO broadening is due to an impurity potential $\sim \hbar/\tau_s$. Although there is a lot of scatter on the graph (due to problems in measuring τ_s and the long route to finding T_0) it shows a clear correlation between T_0 and disorder. The linear fit shown has a gradient of 0.95 K ps, which means $\hbar/\tau_s = 8.0k_B T_0$. We note the similarity between this factor and the fact that Eq. (2) predicts SdHO minima will be $\sim 50\%$ developed when $k_B T \sim E_g/6$. This appears to confirm a connection between the collapse of the spin splitting and the disorder potential.

IV. ENERGY GAPS AT ODD INTEGER FILLING FACTORS

We now turn our attention from the spin-split maxima to the minima at odd integral ν and use the temperature dependence of the resistivity there to evaluate the energy gaps at each odd filling factor. As we have previously discussed the data can be analyzed in two ways. Either the actual value of ρ_{xx} at the minimum can be used and an activation energy Δ extracted from an Arrhenius plot, or the depth of the minimum can be used to obtain an energy gap E_g by fitting to the Lifshitz-Kosevich formula Eq. (2). Δ and E_g represent the energy gaps between mobility edges and between Landau level centers respectively and we expect that $E_g = \Delta + \Gamma$, where Γ is the width of the region of extended states. Both Δ and E_g are shown on Fig. 10 for samples G641 and G650. The dashed line on this figure is the single particle Zeeman energy $g_0\mu_B B$. That this is much smaller than the measured energy gaps shows the gaps are dominated by exchange energy. Although there are quite large experimental uncertainties in the measured gaps, especially at large ν , it can be seen that Δ is approximately linear in $1/\nu$ (i.e. magnetic field) and becomes zero at a finite filling factor, giving us a measure of ν_c where the spin gap closes. (These values of ν_c will be discussed in the next section.) The values of E_g measured at magnetic fields above this critical region also appear to be linear in B , with the same slope as Δ but this time extrapolating to the origin. This is consistent with a constant value of Γ that can be obtained from the

negative intercept of the fit to Δ . Near the critical region there is some indication that E_g starts to decrease below the straight line but unfortunately it becomes unmeasurable once $\delta\nu < 0.5$ where there is no longer a clear minimum observable over a range of temperatures. Furthermore, when the gap is collapsing as a function of temperature (as discussed above) the temperature dependence of resistivity can not be used to obtain a value for the gap. We are thus limited to data at temperatures below the point where the maxima start to converge. For $\nu \ll \nu_c$ this is not a problem, but it increases the uncertainty in E_g when $\nu \sim \nu_c$ as there are then fewer suitable points for fitting.

It is important to note that these measurements suggest an energy gap due to exchange that increases *linearly* with magnetic field and is *independent* of temperature once the enhancement is turned on. This allows us to use an effective g -factor that is the same at all fields, and to describe the spin gap as $\Delta_{spin} = g^* \mu_B B$. Furthermore g^* can be obtained from the gradients of the fits shown in Fig. 10 as 6.2 for G650 and 7.6 for G641, values that are generally in agreement with earlier work [11]. Many workers have previously reported such a linear increase [11,14] and found their results puzzling, since simple theories of exchange suggest the gap should increase like \sqrt{B} . This square root dependence arises when the magnetic length $l_B = \sqrt{\hbar/eB}$ represents the average separation of electrons which determines the Coulomb energy $E_c = e^2/4\pi\epsilon_0\epsilon_r l_B$. However, this is only strictly true when there is just one Landau level occupied and the Coulomb energy is small compared with the cyclotron energy. When there are many LLs occupied neither of these conditions are fulfilled: $E_c > \hbar\omega_c$ and only $1/\nu$ of the electrons are able to contribute to the exchange energy as the others are in full LLs. At zero field, and also in the limit of large ν , the correlation length will be set by the Fermi wavevector k_F rather than L_B . These two factors lead to an exchange energy $E_{ex} \sim (e^2/4\pi\epsilon_0\epsilon_r) (k_F/\nu)$ which depends on density and increases linearly with the magnetic field at which each filling factor falls. Thus we can write

$$E_{ex} = \alpha \hbar\omega_c \quad (3)$$

and since $\mu_B = e\hbar/2m_0$, with m_0 the free electron mass and m^* the effective mass, α is related to the g -factor by:

$$\alpha = (g^* - g_0) \frac{m^*}{2m_0} \quad (4)$$

Aleiner and Glazman [15] have used a more sophisticated Hartree-Fock calculation with Thomas-Fermi screening to show that exchange energy should increase linearly with magnetic field in the large filling factor limit, but that there is an additional logarithmic factor such that $\alpha = (1/\pi k_F a_B) \ln(2k_F a_B)$, where a_B is the effective Bohr radius. Thus α is predicted to vary with carrier density since, with n_e in units of $10^{15} m^{-2}$, $k_F a_B = 1.13\sqrt{n_e}$ giving a value of $\alpha = 0.23$ at $n_e = 10^{15} m^{-2}$. While FS use this value of α in their calculation they do not seem to account for its density dependence.

The values of g^* obtained for each sample from the gradients of plots such as Fig. 10 are shown as a function of $n_e^{-1/2}$ in Fig. 11. This figure clearly shows that there is a density dependence of g^* and that it is somewhat weaker than $n_e^{-1/2}$. The dotted and the dashed lines given by the equations $g^* = g_0 + 6.27/\sqrt{n_e}$ and $g^* = g_0 + 6.22/\sqrt{n_e} + 1.88 \ln(\sqrt{n_e})/\sqrt{n_e}$ represent the simplest and the best fits to the data respectively, which have been constrained to pass through $g^* = g_0$ at large density. By contrast the dash-dotted line is the prediction of

Ref. [15] ($g^* = g_0 + 6.75/\sqrt{n_e} + 8.29 \ln(\sqrt{n_e})/\sqrt{n_e}$), which does not fit the data particularly well and produces an unexpected maximum. The discrepancy is mostly due to an over estimate of the logarithmic correction, and apart from this numerical factor the experiment and theory are in reasonable agreement.

V. THE CRITICAL FILLING FACTOR — ν_C

Having discussed something of the temperature dependence of the spin splitting we can now establish a reliable way of obtaining the critical filling factor ν_c at $T = 0$, which is the quantity required for comparison with the theory of FS. The first, and most direct, approach is to follow the temperature dependence of the separation $\delta\nu$ between the spin split maxima. The crudest method of finding ν_c is by extrapolation of the temperatures where $\delta\nu = 0.5$ on Fig. 5 to $T = 0$. The problem with this approach is that the value obtained is sensitive to the functional form chosen for the curve, particularly if the experimental data does not extend to sufficiently low temperature.

A more accurate method is to plot the values of $T_{0.5}$ as a function of $1/\nu$ and extrapolate to $T = 0$ as shown in Fig. 12. This graph shows a linear dependence with the intercept giving the critical filling factor at $T = 0$, of 23 for this sample. From these data it is quite clear that at $T = 0$ the spin splitting will collapse at a certain magnetic field as opposed to tailing off exponentially. A similar approximately linear relationship is observed for all the samples and so we propose the empirical relationship:

$$\frac{1}{\nu_c(T)} = \frac{1}{\nu_c(0)} + cT \quad (5)$$

with c and $\nu_c(0)$ as sample dependent parameters. These parameters will be discussed in more detail later in the paper, but at this point it is important to note that there is no direct correlation between them. This means that $\nu_c(0)$ can not be obtained just by finding the last spin split maximum in a single finite temperature resistivity trace. There is sometimes a deviation from linearity at the lowest filling factors $\nu = 3$ or 5, with values of $T_{0.5}$ up to 20% below the line. This may be an artifact of the experiment since the transition region occurs above 1 K where the temperature in the fridge was not always stable. Alternatively it may provide evidence for skyrmionic excitations at these filling factors having a correspondingly lower energy than the single spin flips. In any case we have not used these points in our analysis of ν_c .

The critical filling factor can also be obtained from the point where the mobility gap Δ collapses, via the temperature dependent resistivity data discussed in the previous section. The values of ν_c obtained from the two methods are very similar, although for the cleanest samples the collapsing of the gap gives slightly smaller values. This may be due to the difficulty in measuring small energy gaps and for the remainder of the paper we will use the former method.

A. Sample dependence of ν_c

Having established a method of finding the $T = 0$ value of ν_c we can now investigate how it varies between samples. In their calculations Fogler and Shklovskii [6] found different

expressions for the dependence of ν_c on sample parameters according to the range of the dominant scattering mechanism in each case. For low mobility samples they found $N_c \propto n_e \mu$ and for high mobility samples $N_c \propto L_z n_e^{5/6} / n_i^{1/3}$, with electron densities in our range of interest and similar forms of expressions for other densities. These predictions are tested by plotting our measured ν_c against $n_e \mu$ and $L_z n_e^{5/6}$ in Fig. 13. Clearly there are some samples that agree with the predictions in each case but neither description applies to all the samples and there is no clear distinction between the low and high mobility samples. This lack of agreement is not unexpected since our samples cover a wide range of densities and mobilities and different scattering mechanisms will dominate. In drawing these figures we have also to assume that the impurity density n_i is constant, as there is no way of measuring this directly, but in practice it may differ widely between the samples. However, in FS all the sample parameters enter through the calculation of the scattering rate τ_s . Rather than try to calculate this quantity we will show that the theory is essentially correct by using the measured value of τ_s , obtained from the SdHOs at low magnetic field.

Simply speaking the spin splitting will collapse when the energy separation of spin up and down levels is less than their disorder broadening *i.e.* when

$$g^* \mu_B B = \hbar / \tau_s. \quad (6)$$

At this point the exchange contribution will disappear and only the small bare Zeeman splitting will remain. Rearranging this equation in terms of the critical filling factor and electron density we obtain

$$\nu_c = g^* n_e \tau_s \frac{\hbar}{2m_0} \quad (7)$$

The $T = 0$ values of ν_c are plotted as a function of $g^* n_e \tau_s$ in Fig. 14, together with the prediction of Eq. (7). Clearly this provides a good description for all the samples without using any adjustable parameters. There are quite large experimental uncertainties in the measurement of both g^* and τ_s indicated by the error bars. (A reliable value of τ_s could not be obtained for sample G627 because the magnetic field was swept too fast to resolve the SdHOs at low field. However, ν_c for this sample is quite in line with the value expected.) It is quite remarkable how well this very simple approach matches the experimental data particularly that the disorder broadening seems to be adequately described by \hbar / τ_s without any numerical factors.

Returning to Eq. (5), it can be seen that not only did the critical filling factor at $T = 0$ vary between the samples, but so did the rate of change of critical filling factor with temperature. We will now try to understand this temperature dependence in another simple model. As the temperature is increased, reversed spins will be thermally excited, which will reduce the exchange correlation. Thus the exchange enhancement can be destroyed even when $g^* \mu_B B > \hbar / \tau_s$. We propose the critical condition for the spin splitting to collapse at finite temperature to be

$$g^* \mu_B B = \hbar / \tau_s + M k_B T \quad (8)$$

where M is a numerical constant that determines the effect of the thermal fluctuations on the exchange energy. Comparing this with Eq. (5), and using Eq. (7) to replace τ_s

with $\nu_c(0)$, shows that the parameters c and M that we have introduced are related by $c = Mk_B m_0 / \pi \hbar^2 n_e g^*$, *i.e.* just fundamental constants and the sample dependent product $n_e g^*$. In Fig. 15 the linear dependence of $1/c$ on this product is very clear and from the slope of this graph we obtain a value of $M = 2.1$ which appears quite reasonable. Again it is remarkable how well this simple model, of thermally excited spins aiding the disorder potential in destroying the exchange correlation, accounts for the data. A full theory is required to account for the actual value of M .

VI. TILTED MAGNETIC FIELD AND THE ENHANCED g -FACTOR

It is well known that for a 2DEG the cyclotron motion, and hence the energy $\hbar\omega_c$, and the magnetic length, only depend on the perpendicular component of B whereas the Zeeman energy depends on the total magnetic field. This means that on tilting the sample (such that the angle between the magnetic field and a direction normal to the 2DEG is θ) the ratio of the Zeeman to cyclotron energy will increase. When the Zeeman energy is exactly half of the cyclotron energy, at some angle θ_c , a ladder of equally spaced levels is generated and we would expect that the odd and even integer minima in the SdHO have the same depth. At this point we have the condition that $\hbar e B \cos \theta_c / m^* = 2\Delta_{spin}$ which forms the basis for the coincidence method of determining the g -factor [3]. On further tilting other coincidence conditions occur as the levels cross each other. An example of the first condition can be seen in Fig. 16 for sample G650 at very high tilt angles. In the two lower traces the even integer minima are deeper and on further rotation the upper two traces show that the odd integer (spin split) minima dominate, allowing us to deduce that the coincidence angle is close to $\theta_c = 87.3^\circ$. Notice that this is very close to 90° where the magnetic field is parallel to the 2DEG and $\cos \theta$ is changing very rapidly. In the past the enhanced g -factor has then been extracted by writing $\Delta_{spin} = g^* \mu_B B$ which gives the coincidence condition as

$$\cos \theta_c = g^* \frac{m^*}{m_0} \quad (9)$$

and in this case a value of $g^* = 0.71$. Clearly this is at variance with the value of $g^* = 6.8$ found in Section IV. The same results have also been found in all previous coincidence measurements and various explanations have been given, such as there being less exchange enhancement at high tilt angle or variable degrees of enhancement depending on the occupancies used at the coincidence.

However Eq. (9) is not correct, because Δ_{spin} does not increase linearly with the total field. Although the bare Zeeman part of Δ_{spin} will increase with total field, for an ideal 2DEG the exchange contribution depends only on the perpendicular component so we should write

$$\Delta_{spin} = g_0 \mu_B B_{TOTAL} + \alpha \hbar e B_{\perp} / m^* \quad (10)$$

which leads to a new coincidence condition

$$\cos \theta_c = \frac{g_0}{1 - 2\alpha} \frac{m^*}{m_0}. \quad (11)$$

Using a value of $\alpha = 0.20$ appropriate for G650 with the coincidence at 87.3° gives a value of $g_0 = 0.4$, in good agreement with the bulk band edge value of 0.44. In practice we would

expect a small reduction in the g -factor in the 2-D layer due to the effects of non-parabolicity thus giving even better agreement. Our conclusion therefore is that when analysed in a way which includes the two dimensional nature of the exchange enhancement the coincidence method gives a correct picture of the spin splitting which agrees with other measurements.

To further substantiate the claim that only the bare Zeeman term increases on tilting, we have measured ν_c as a function of tilt angle. The resistivity of sample G650 is shown in Fig. 17 for angles between 0 and 85° as a function of the normal component of magnetic field. This demonstrates that more spin split peaks are observed at higher tilt angles as expected for any mechanism that increases the spin splitting. By following the resistivity at fixed filling factor, it can also be seen that $\delta\nu$ for the spin split maxima displays a very similar behavior as a function of tilt to that found earlier as a function of temperature. In the tilting case, the additional parallel field should be considered to open up the spin gap by increasing the bare Zeeman contribution, thus delaying the disorder driven collapse just as increasing temperature hastened this collapse by adding to the spin disorder. In Ref. [9] the critical density was found to decrease at higher tilt angles which is equivalent to saying that the point of collapse moves to lower magnetic fields and is entirely consistent with our results.

When only the bare Zeeman energy increases on tilting, the critical filling factor is given by

$$\nu_c(\theta) = n_e \tau_s h \left(\frac{g_0}{2m_0 \cos \theta} + \frac{\alpha}{m^*} \right) \quad (12)$$

where it can be seen that the increase in ν_c with angle is only due to the first term – the contribution from the bare Zeeman energy. The measured critical filling factor is shown as a function of tilt in Fig. 18 for sample G650. The line drawn on this figure has the gradient predicted by Eq. (12), using $g_0 = 0.40$, with an intercept for ν_c slightly lower than deduced in section V due to the finite temperature of the measurement. The agreement between the theory and experiment clearly demonstrates that only one part of the spin splitting is increasing as the field is tilted, as otherwise the gradient would depend on g^* and be some 15 times larger. At the highest angles the data begins to fall below the line. The most likely cause of this is a reduction in τ_s caused by the parallel field which will push the wavefunction closer to the interface increasing the scattering. For angles above 85° there is also a large positive magnetoresistance, suggesting a change in scattering. However, we were not able to verify this directly by measuring τ_s at high tilt angles, precisely because the SdHOs are spin split to much higher filling factors.

Several papers have previously measured activation energies in tilted fields in an attempt to extract the enhanced g -factor from the rate of change of energy gap with tilt angle. The new analysis presented above suggests however that accurate and consistent results can only be achieved by including the two dimensional nature of the exchange interactions.

VII. CONCLUSION

In this paper we have considered how the spin splitting is increased by the addition of an exchange term to the bare Zeeman energy. This enhancement is only present when the spin gap is larger than the disorder potential in the sample which can be parameterized by

τ_s . Once the exchange enhancement can no longer be sustained the spin splitting collapses critically, which is seen both by the separation in filling factor $\delta\nu$ of the spin split maxima and the energy gap deduced from the depth of the minima. We have examined the filling factor ν_c at which this critical collapse occurs as a function of temperature. Increasing the temperature leads to a lower value of ν_c because thermally excited spins essentially add to the disorder potential that the exchange energy must exceed. A scaling behavior is found which maps the temperature dependence of $\delta\nu$ for all filling factors in all the samples on to a single curve. A reliable method of extracting the critical filling factor at $T = 0$ from finite temperature data is established. By investigating the variation of ν_c at zero temperature between samples we find a universal empirical relationship $\nu_c = g^*n_e\tau_s h/2m_0$ which is completely consistent with the picture of disorder driven collapse. In tilted magnetic field experiments, ν_c increases as the component parallel to the 2DEG is increased. This is found to be due to only the bare Zeeman component of the spin splitting increasing, not the exchange term. This finding allows us to understand past discrepancies between different methods of measuring the enhanced g -factor.

ACKNOWLEDGEMENTS

We would like to thank H. Aoki, G.Kido, D.M. Symons and S. Uji for assistance at NRIM, Tsukuba, in making the tilted field measurements.

REFERENCES

- [1] K. von Klitzing, M. Dorda and M. Pepper, (1980)
- [2] T. Ando, A.B. Fowler and F. Stern, *Rev. Mod. Phys.* **54** 545 (1982) and refs. therein.
- [3] R.J. Nicholas, R.J. Haug, K. von Klitzing and G. Weimann, *Phys. Rev. B* **37**, 1294 (1988) and refs. therein.
- [4] T. Ando and Y. Uemura, *J. Phys. Soc. Jpn.* **37**, 1044 (1974)
- [5] C. Kallin and B.I. Halperin, *Phys. Rev. B* **30**, 5655 (1984)
- [6] M.M. Fogler and B.I. Shklovskii, *Phys. Rev. B* **52**, 17366 (1995)
- [7] S.L. Sondhi, A. Karlhede, S.A.. Kivelson and E.H. Rezayi, *Phys. Rev. B* **47**, 16419 (1993); H.A. Fertig *et al.* *Phys. Rev. B* **50**, 11018 (1994); S.E. Barret *et al.* *Phys. Rev. Lett.* **74**, 5112 (1995); E.H. Aifer *et al. ibid.* **76**, 680 (1996)
- [8] N.R. Cooper, *Phys. Rev. B* **55**, R1934 (1997)
- [9] L.W. Wong, H.W. Jiang, E. Palm and W.J. Schaff, *Phys. Rev. B* **55**, R7343 (1997)
- [10] R. Shikler, M. Heiblum and V. Umansky, *Phys. Rev. B* **55**, 15427 (1997)
- [11] A. Usher, R.J. Nicholas, J.J. Harris and C.T. Foxon, *Phys. Rev. B* **41**, 1129 (1990)
- [12] D. Shoenberg, *Magnetic oscillations in metals* Cambridge University Press, (1984)
- [13] We will usually refer to the filling factor rather than the LL index. They are related by $\nu = 2N + 1$ so $\nu = 1$ is the spin split minimum of the $N = 0$ LL etc.
- [14] V.T. Dolgoplov, A.A. Shashkin, A.V. Aristov, D. Schmerek, W. Hansen and M. Holland, *Phys. Rev. Lett.* **79**, 729 (1997)
- [15] I.L. Aleiner and L.I. Glazman, *Phys. Rev. B* **52**, 11296 (1995)

TABLES

TABLE I. Sample parameters (after illumination, except where marked *): spacer thickness L_z ; electron density n_e and mobility μ at 1 K; quantum lifetime τ_s deduced from Eq. (2). g^* and ν_c are discussed in the text.

Sample	L_z Å	n_e $\times 10^{15} m^{-2}$	μ m^2/Vs	τ_s ps	g^*	ν_c
G647	3200	0.45	245	6.7	8.5	11
G646	2400	0.63	200	10.5	7.3	21
G641	1600	0.90	400	13.0	7.6	31
G137	1600	0.99	100	4.0	6.3	15
G640	1200	1.2	680	7.3	6.5	23
G650	400	2.2	630	6.3	6.2	29
G627*	400	2.0	310	-	-	17
G627	400	3.0	370	-	-	35
G902*	200	3.1	148	1.1	5.1	11
G902	200	4.5	200	2.0	4.2	20
G590*	100	3.2	12	0.7	4.0	5
G590	100	6.1	65	0.9	3.4	10
G378	100	3.4	6	0.4	3.4	3

FIGURES

FIG. 1. Magnetoresistance of sample G641 at 90 mK showing the spin splitting collapse as a function of magnetic field.

FIG. 2. The data from Fig. 1 replotted as a function of filling factor together with data taken at 230 mK and 600 mK which show how ν_c decreases at higher temperature.

FIG. 3. Magnetoresistance of sample G590 at several temperatures, showing a critical collapse of the spin splitting at $\nu = 11$ (2.5 T). The insert shows well resolved SdHOs to $\nu > 70$.

FIG. 4. Spin splitting at $\nu = 15$ for sample G902, showing how the maxima converge and the gap collapses as the temperature increases from 40 mK to 1 K

FIG. 5. Temperature dependence of the filling factor at which spin split maxima occur in sample G640. The dashed line, drawn through the positions where $\delta\nu = 0.5$, defines the boundary between spin resolved and unresolved phases.

FIG. 6. Separation of each spin split maxima $\delta\nu$ for sample G902 as a function of temperature.

FIG. 7. The data from the previous figure showing a single curve as a function of $T - T_{0.5}$, where $T_{0.5}$ is the temperature at which $\delta\nu = 0.5$ at each filling factor.

FIG. 8. Universal behavior of $\delta\nu$ for all samples and all ν appears with the temperature suitably scaled. T_0 is a sample dependent scaling parameter, which corresponds to the temperature range over which the spin gap collapses.

FIG. 9. Variation of the sample dependent scaling temperature T_0 with disorder, parameterised as the inverse quantum lifetime.

FIG. 10. Energy gaps at odd integer filling factor for samples (a) G650 and (b) G641. The fitted lines are discussed in the text. The dashed line is the single particle Zeeman energy.

FIG. 11. Density dependence of the measured effective g -factor. The dotted and dashed curves are fits to the data described in the text and the dot-dashed line is the theory of Ref. 15

FIG. 12. Variation of ν_c with temperature for sample G640. The intercept of the straight line fit gives the critical filling factor at $T = 0$.

FIG. 13. Test of the dependence of ν_c on the sample parameters predicted by FS and discussed further in the text.

FIG. 14. The critical filling factor as a function of the product $g^*n_e\tau_s$, obtained from measuring each parameter, showing excellent agreement with the prediction of Eq. (7).

FIG. 15. Sample dependence of the parameter c , determined from the gradients of plots like Fig. 12.

FIG. 16. SdHOs at very high tilt angles θ to the sample normal, showing the swap in intensity between even and odd integer ν and their coincidence at $\theta = 87.3^\circ$.

FIG. 17. SdHOs for sample G650 in tilted fields at the angles indicated. Note how the spin split minima are deeper and ν_c increases at higher tilt angles.

FIG. 18. Variation of the filling factor at which spin splitting collapses as a function of tilt angle for sample G650.

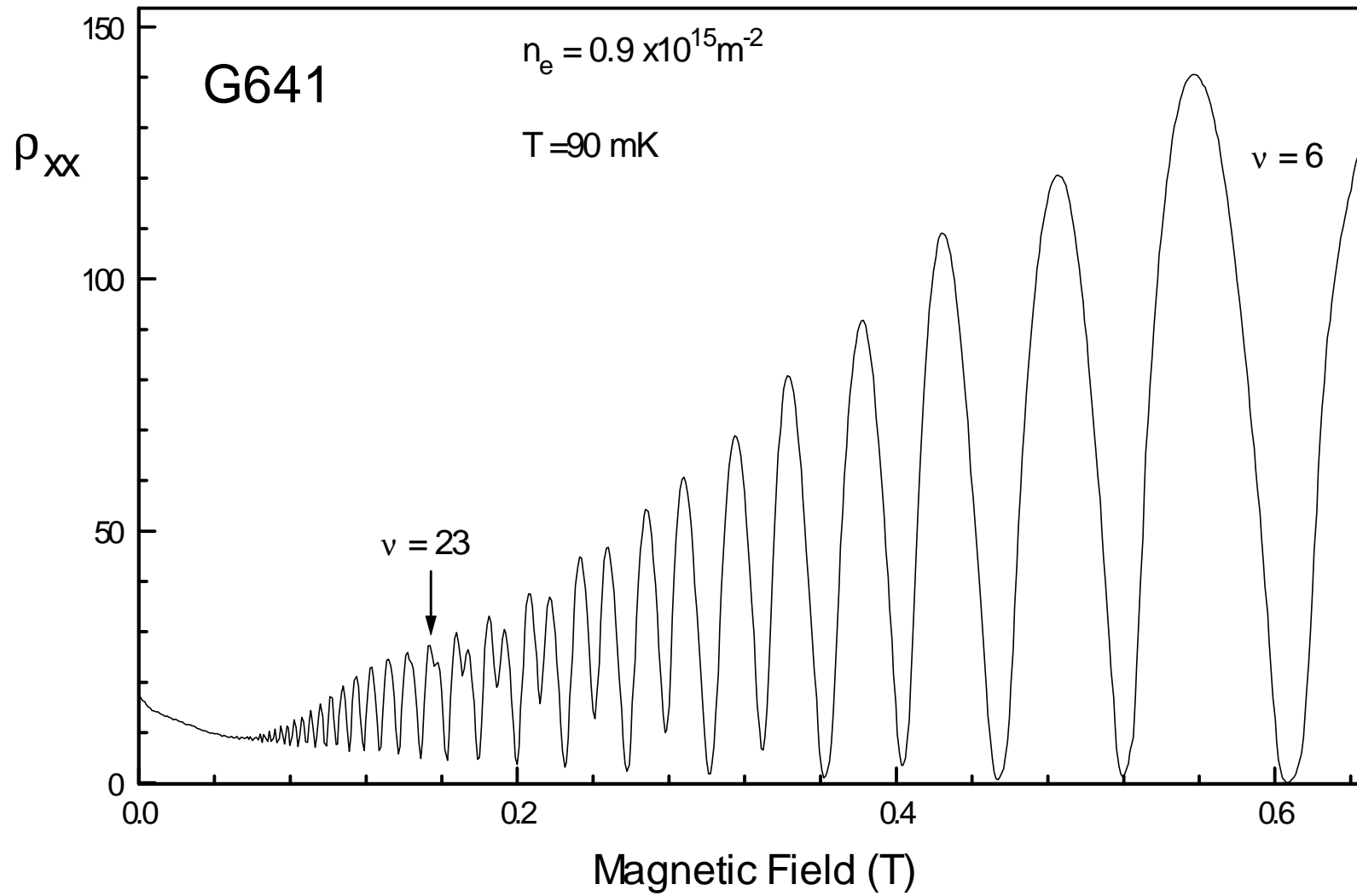


Figure 1

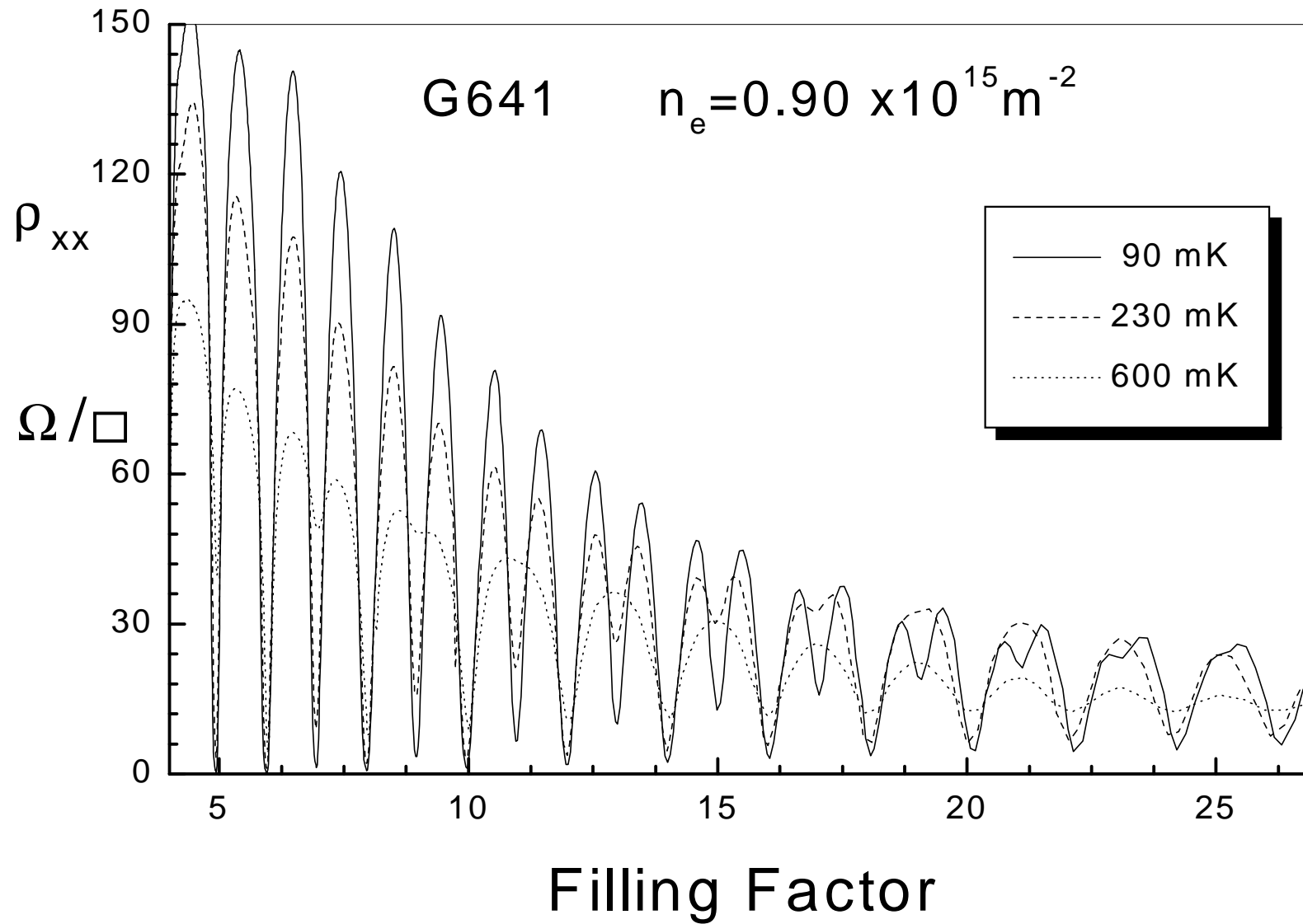


Figure 2

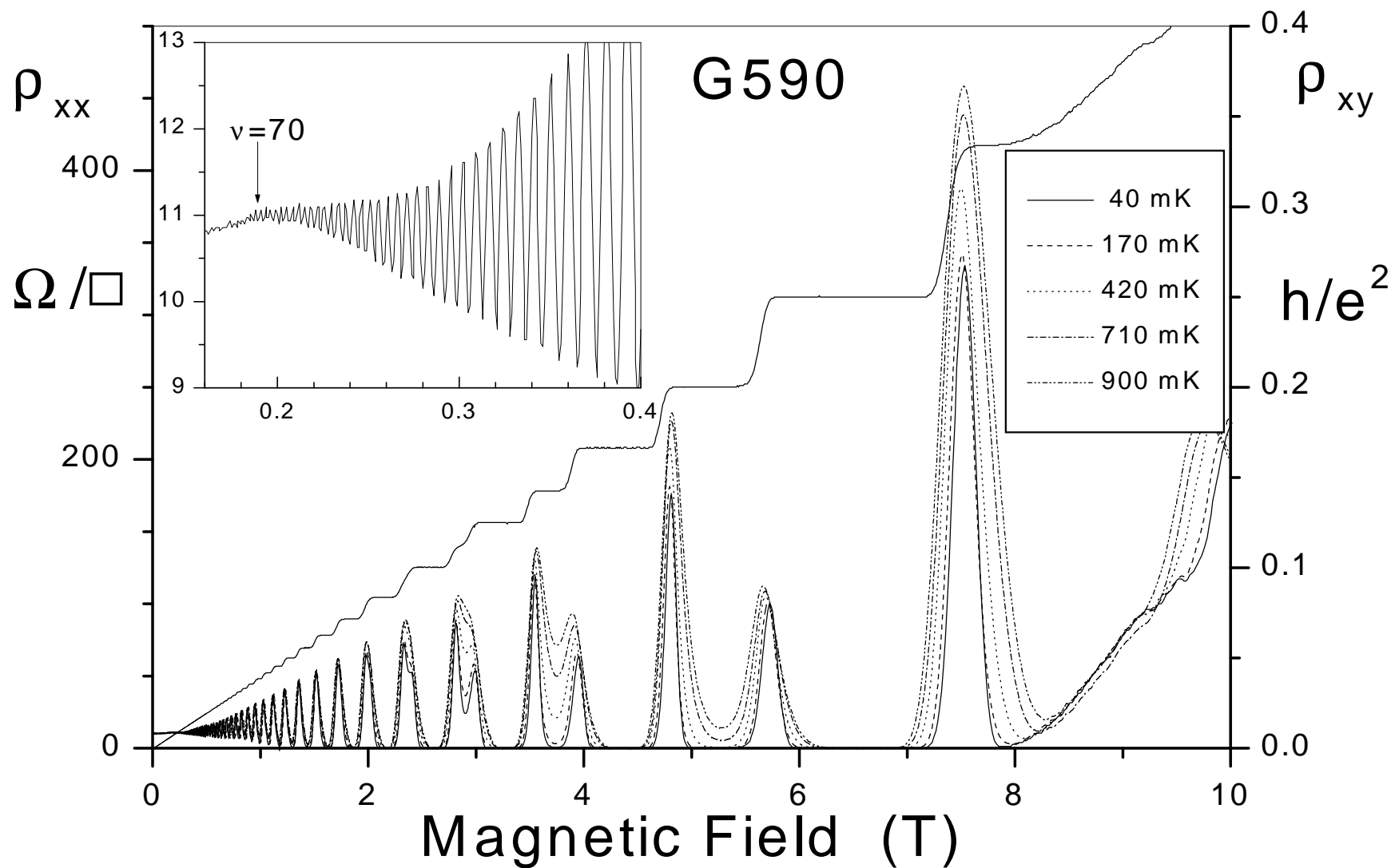


Figure 3

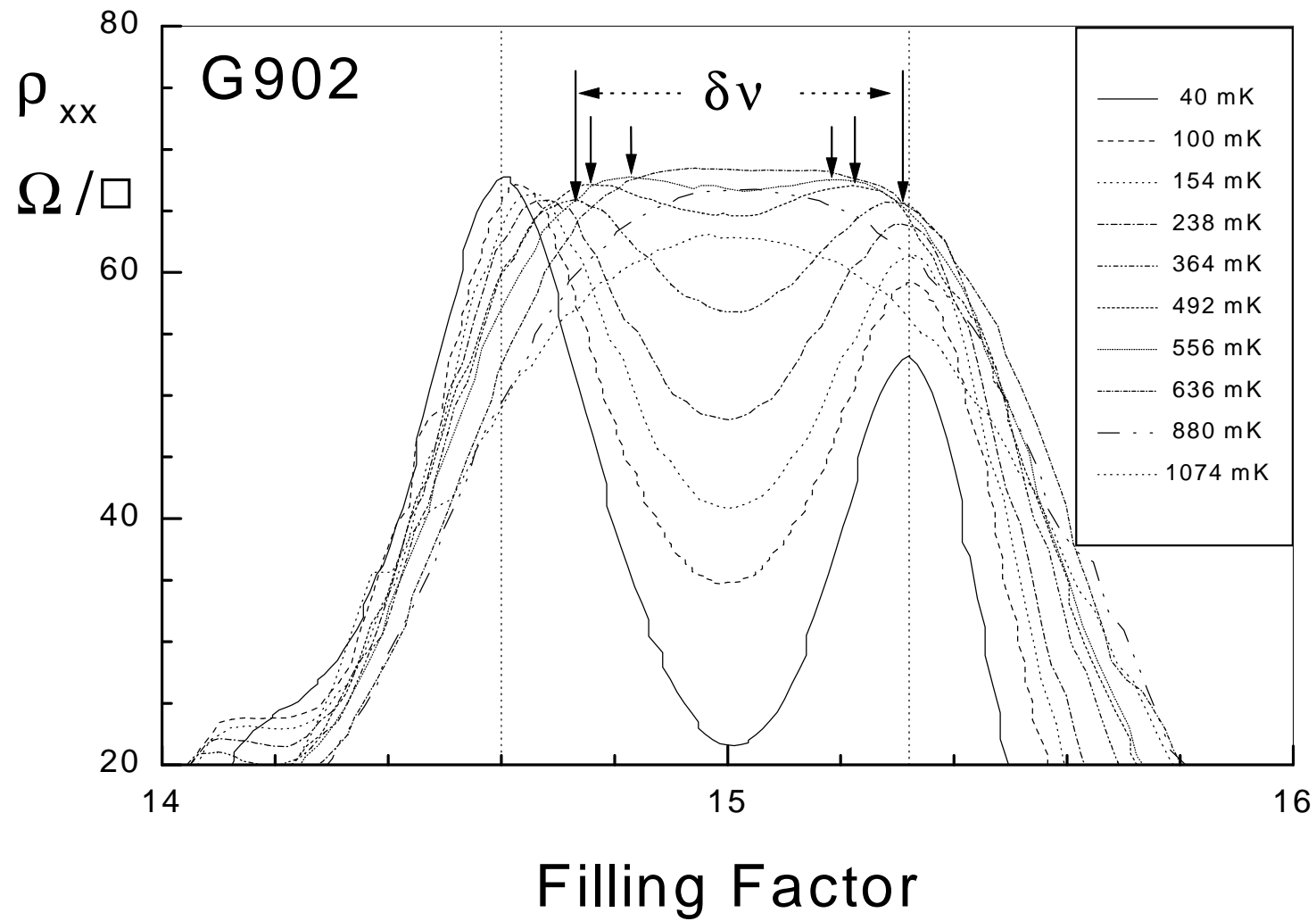


Figure 4

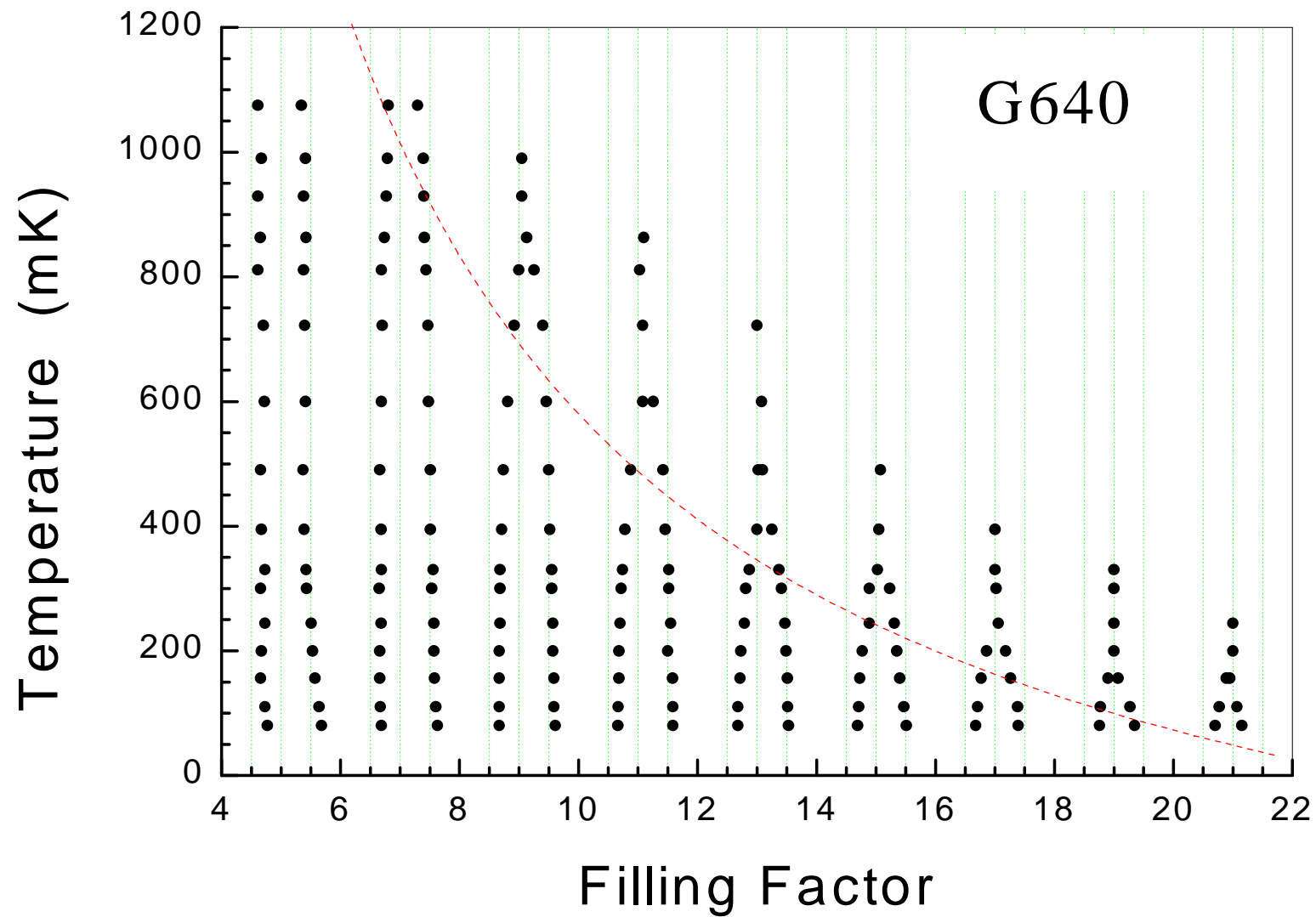


Figure 5

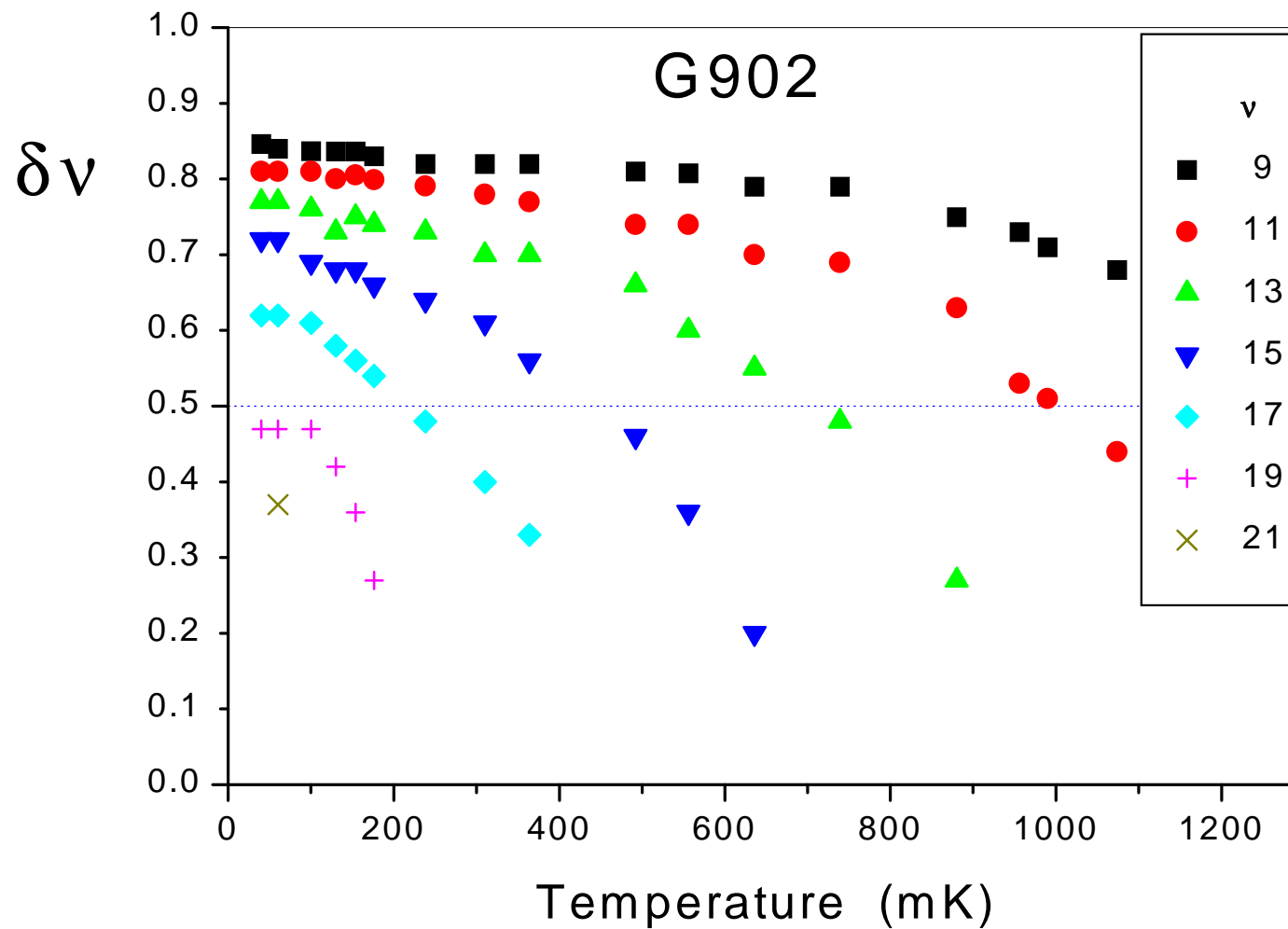


Figure 6

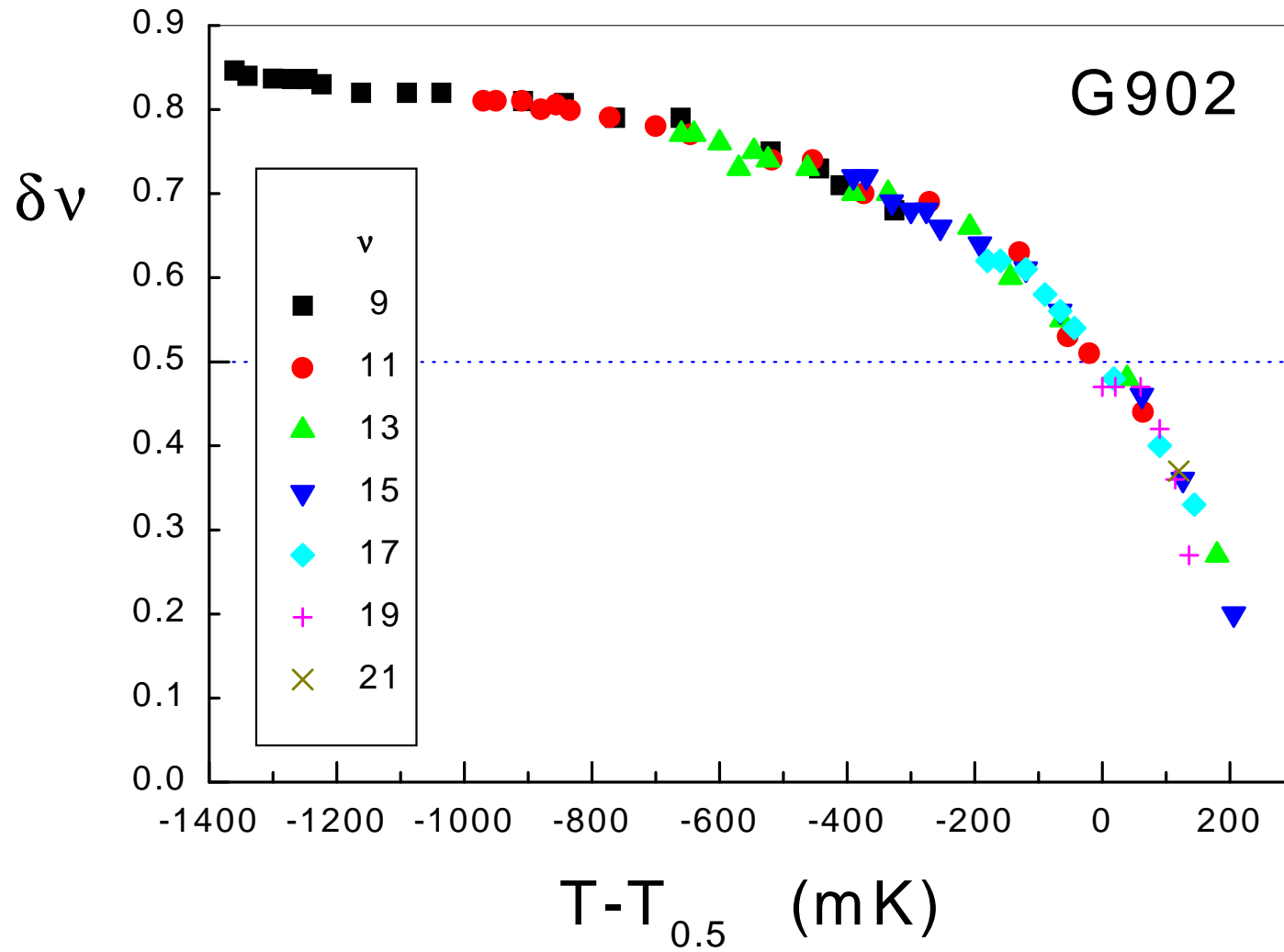


Figure 7

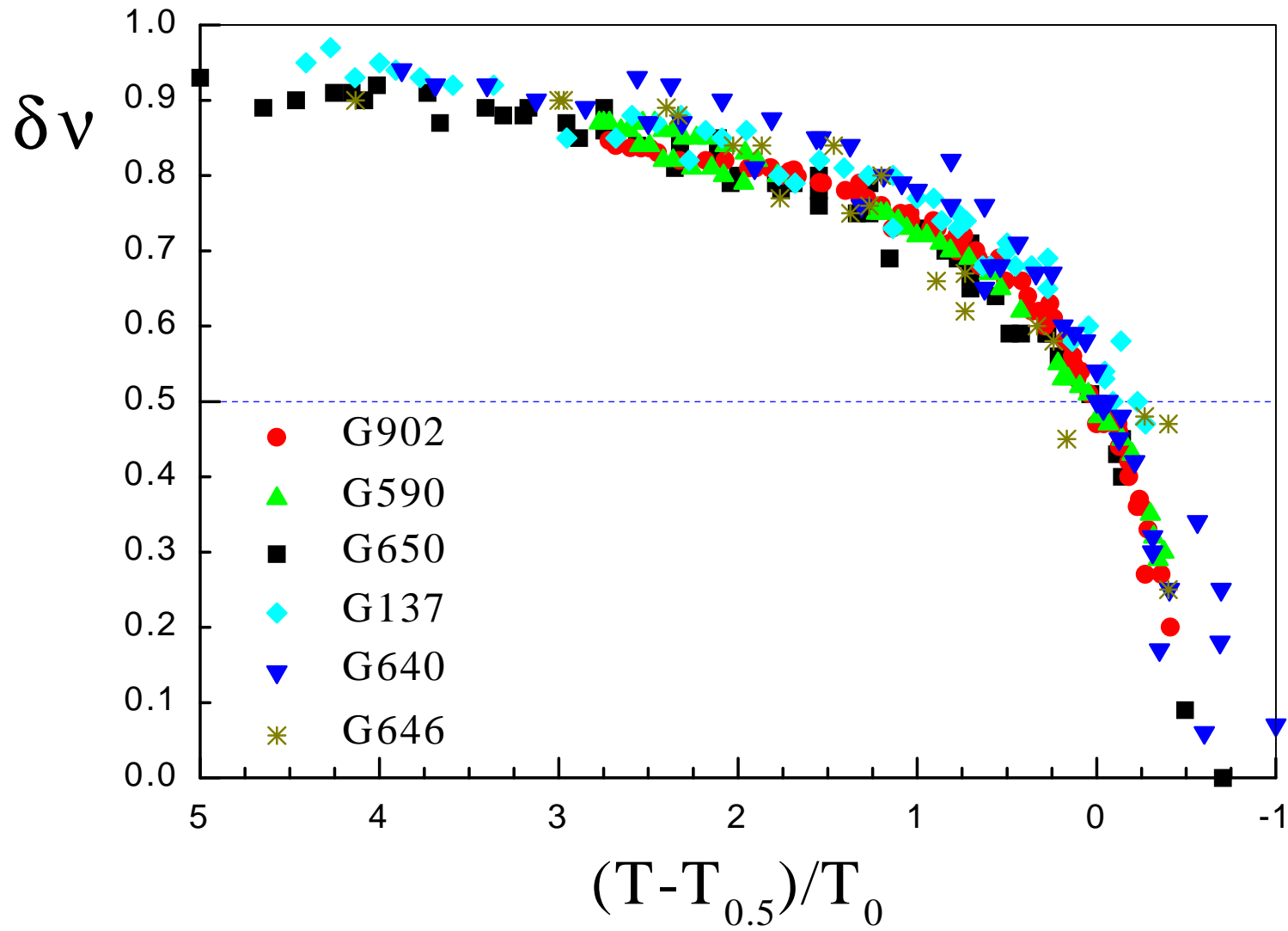


Figure 8

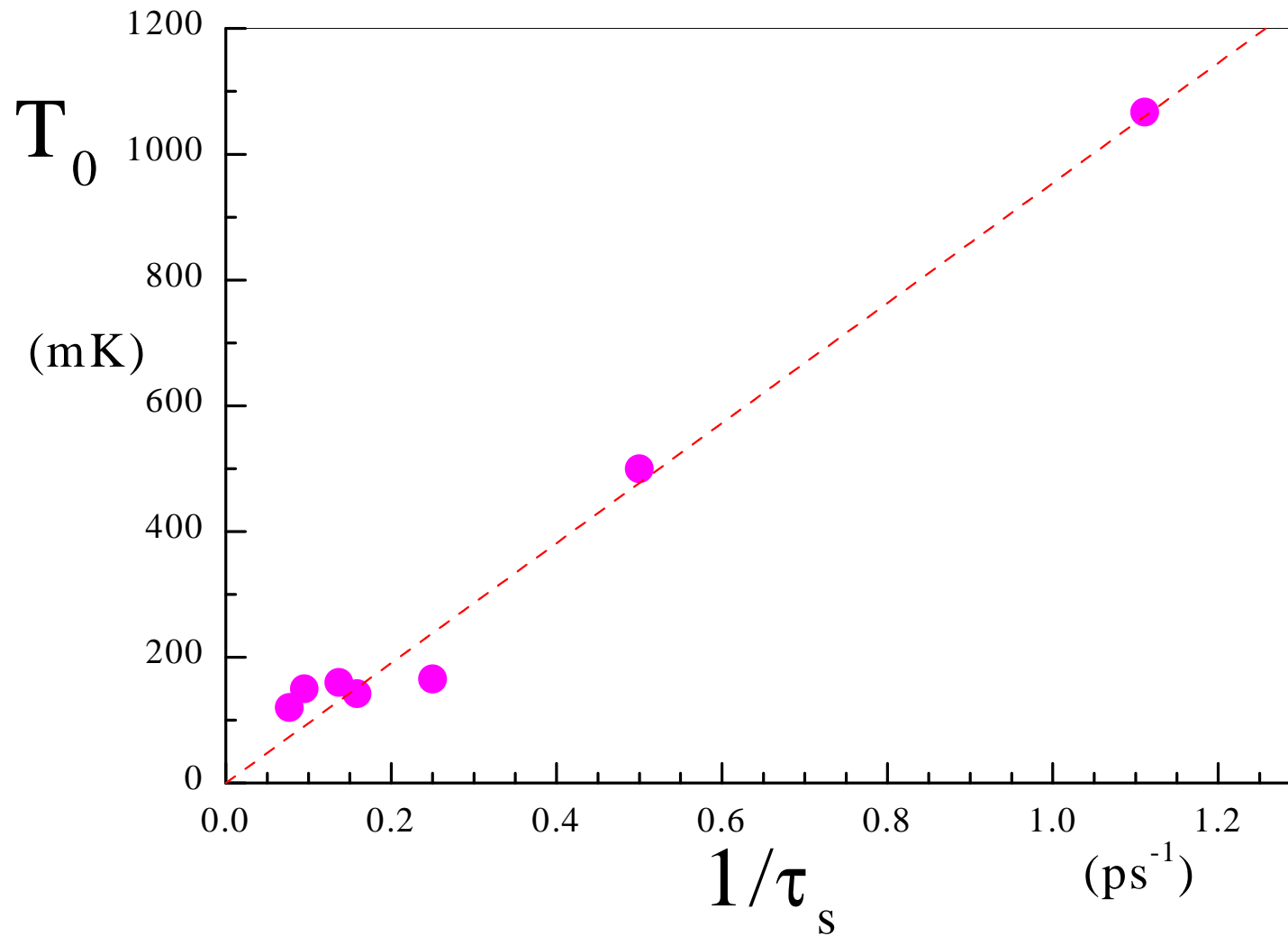


Figure 9

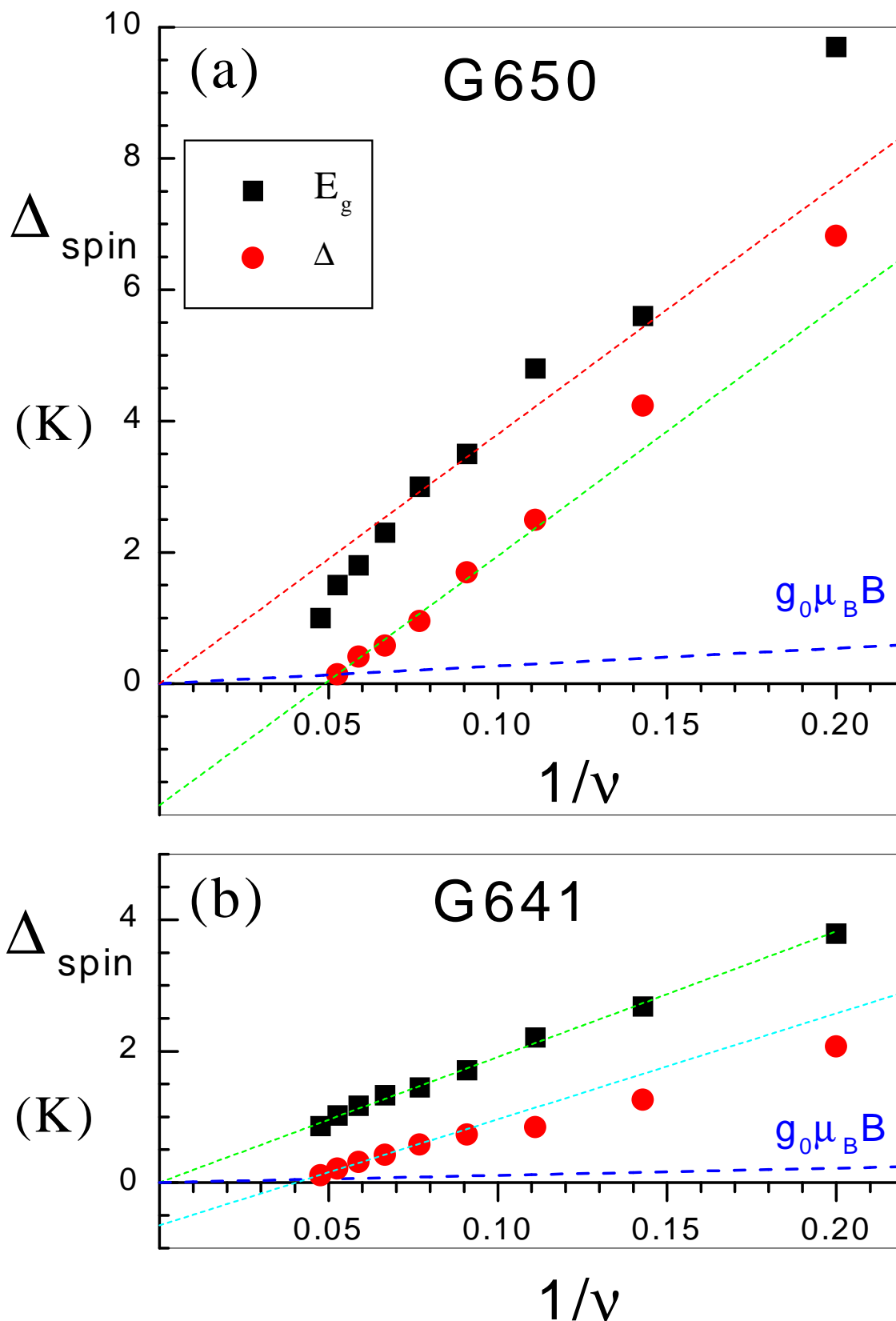


Figure 10

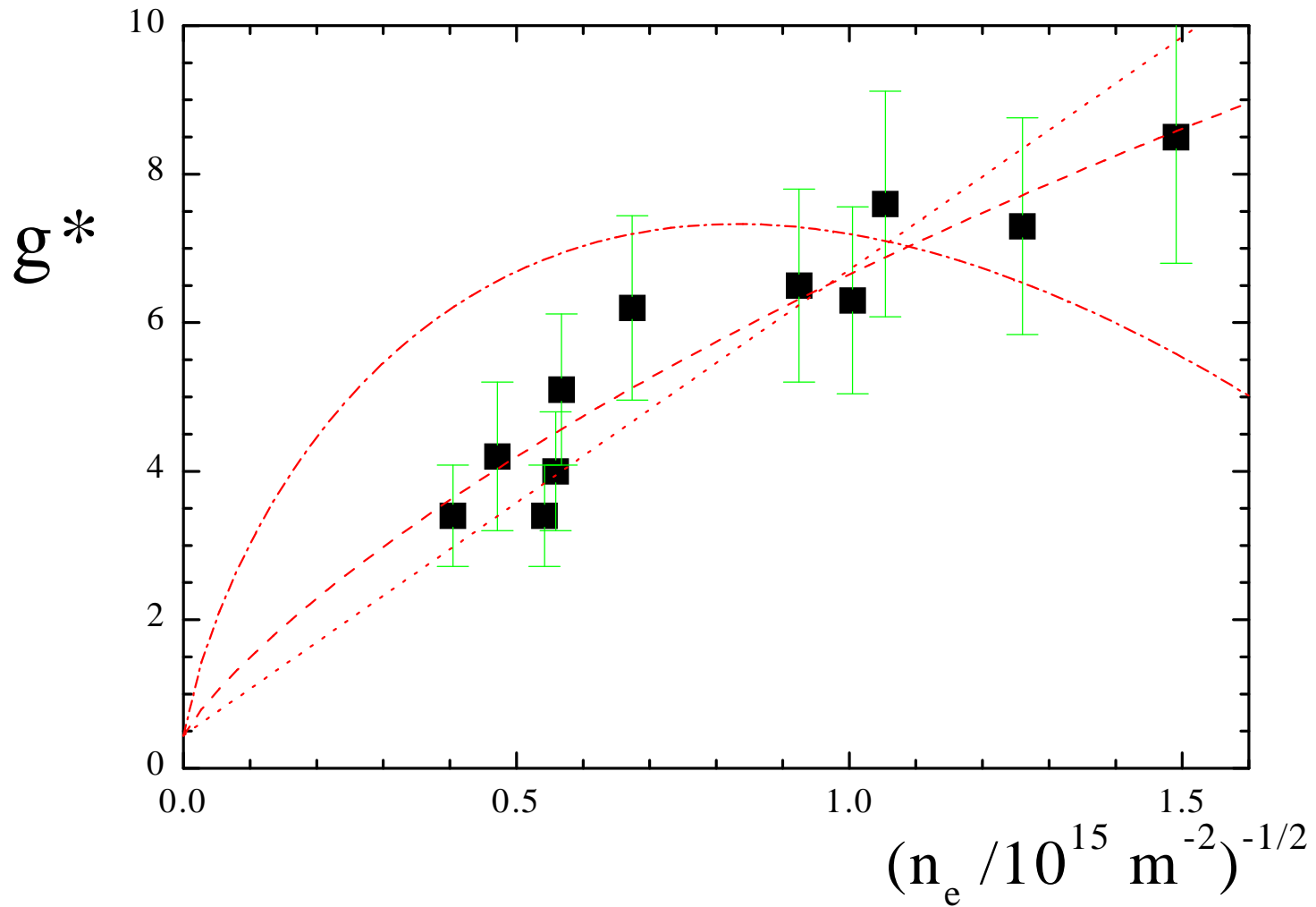


Figure 11

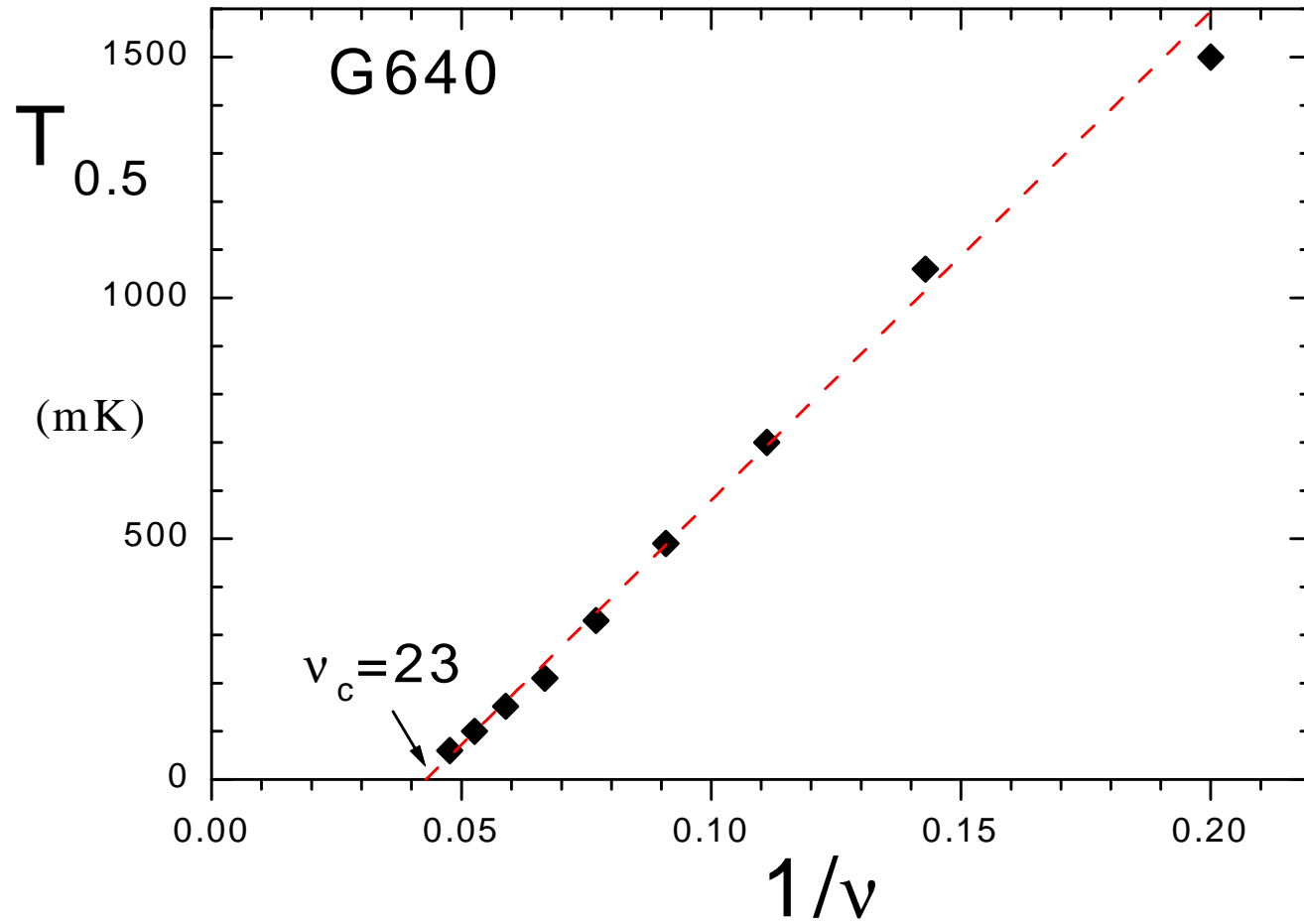


Figure 12

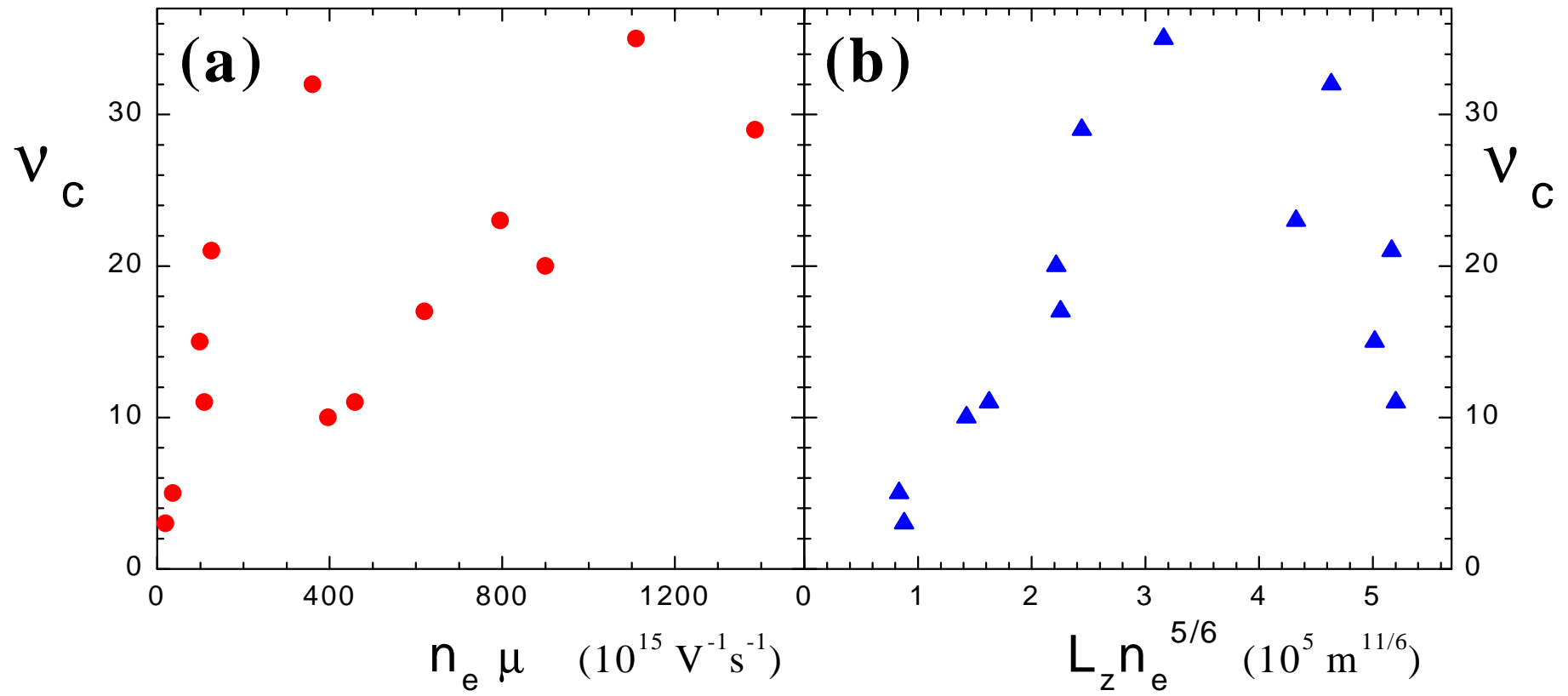


Figure 13

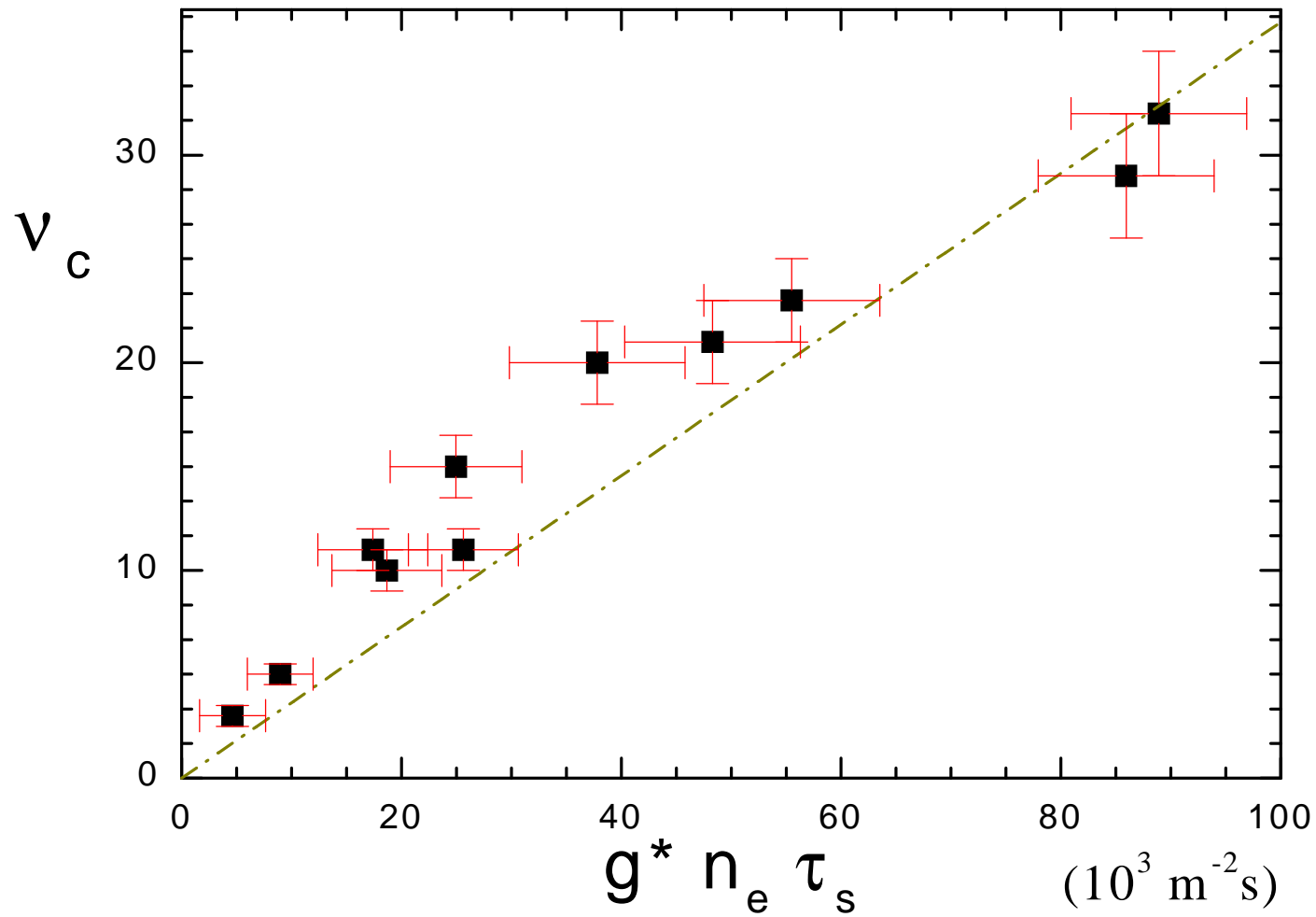


Figure 14

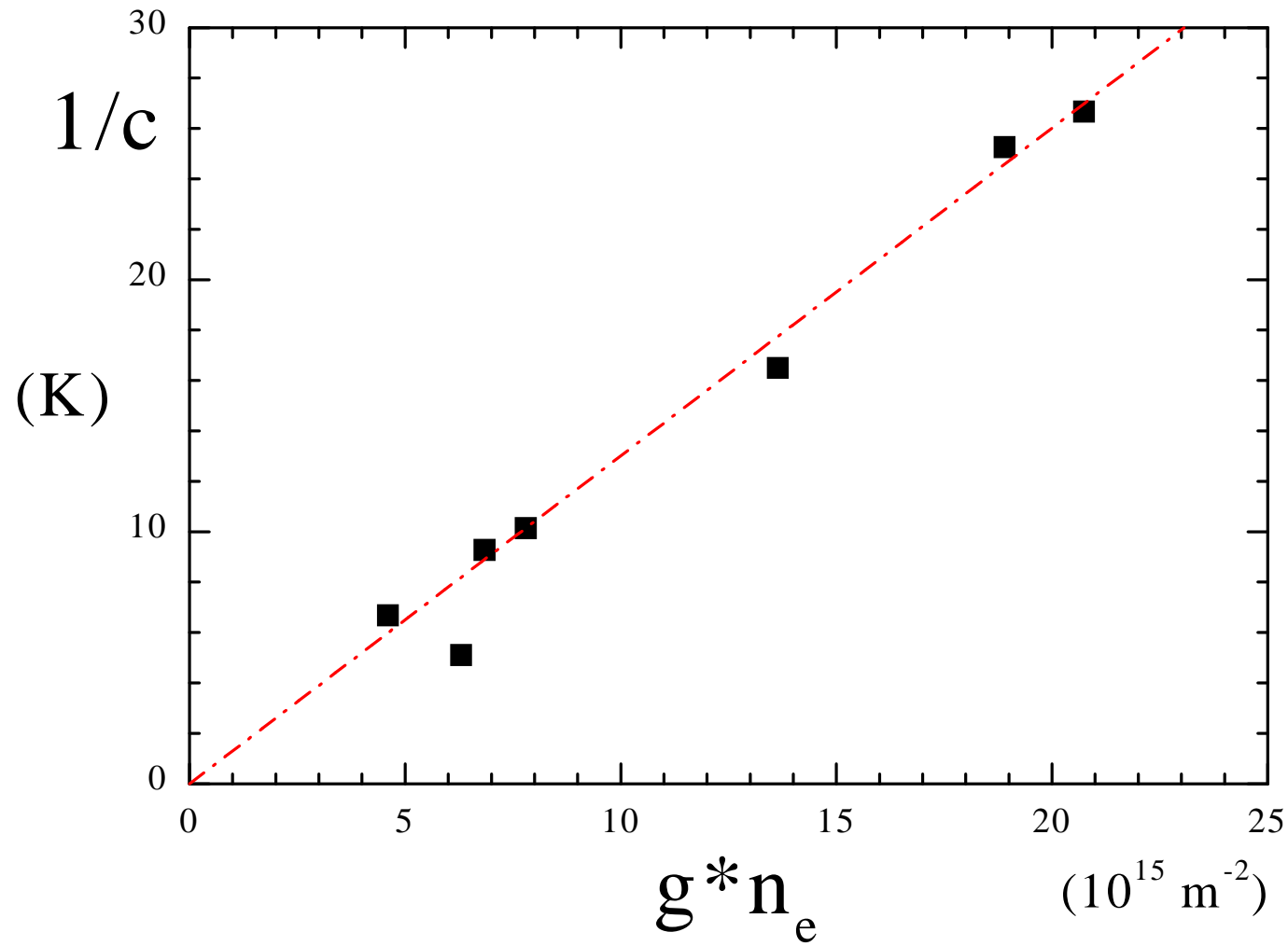


Figure 15

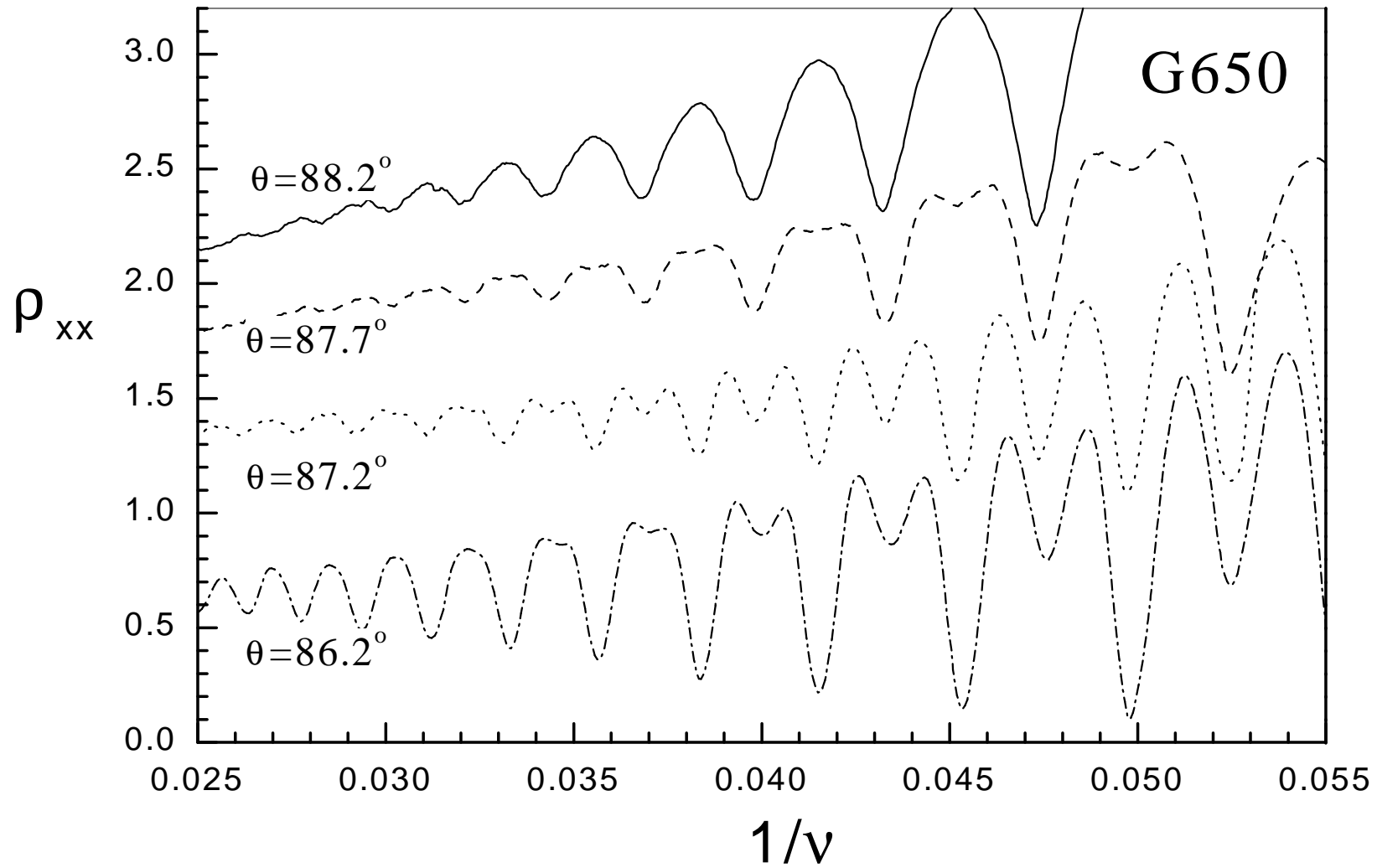


Figure 16

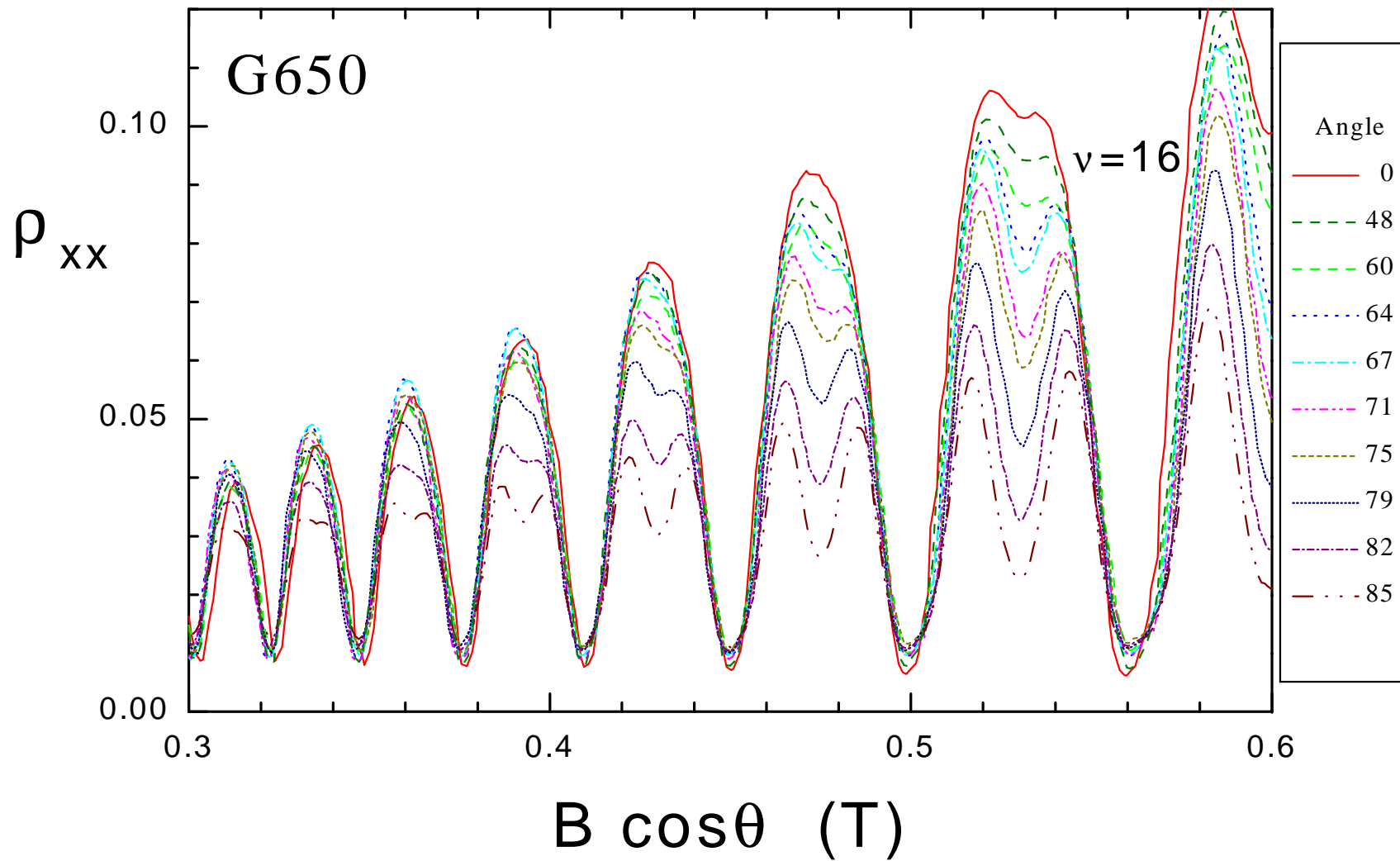


Figure 17

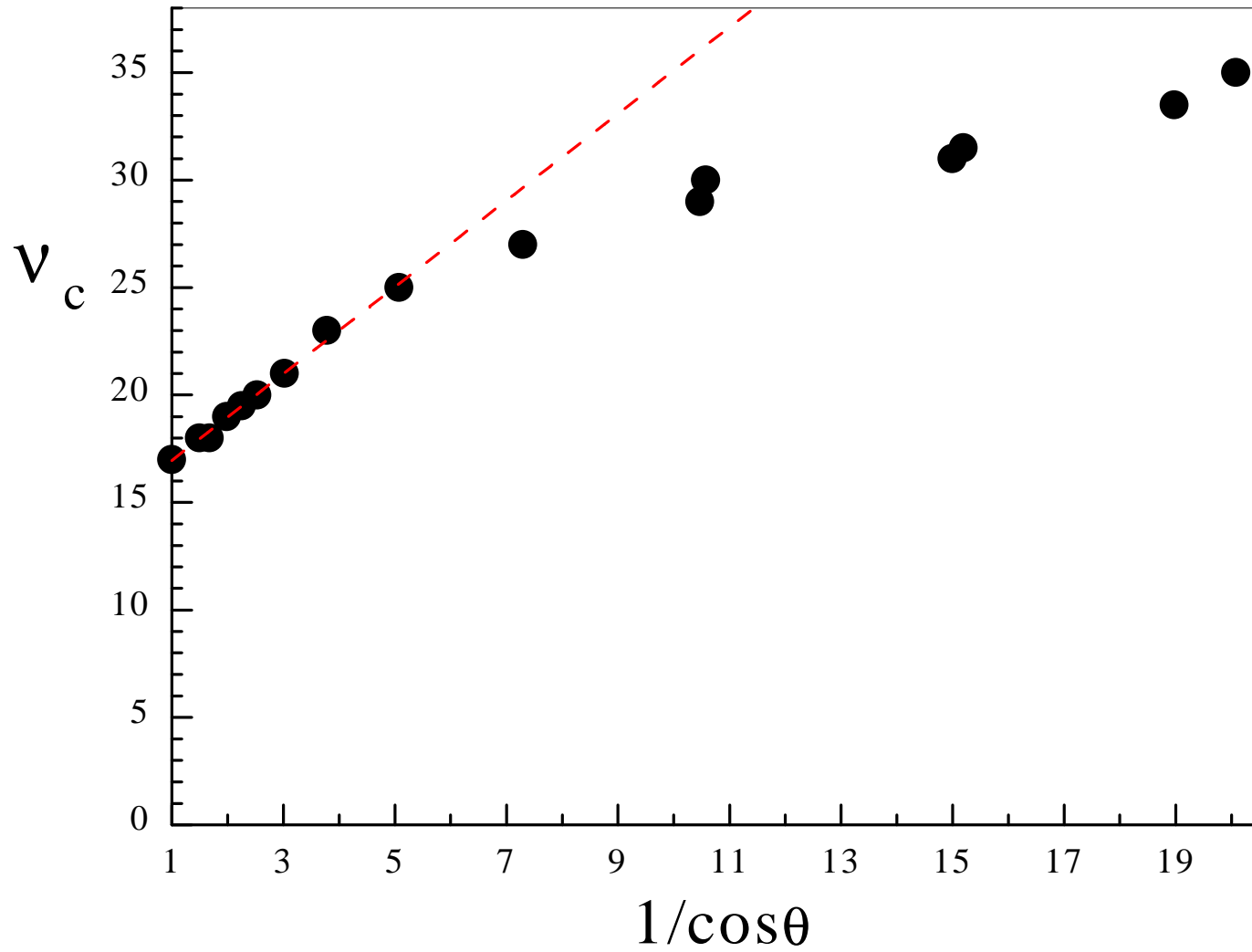


Figure 18